Study of hard x-ray emission from intense femtosecond Ti:sapphire laser–solid target interactions

L. M. Chen, P. Forget, S. Fourmaux, and J. C. Kieffer
INRS-Energie, Matériaux et Télécommunications, Université du Québec, Varennes (Quebec) J3X 1S2, Canada

A. Krol and C. C. Chamberlain
Upstate Medical University, SUNY, Syracuse, New York 13210

B. X. Hou, J. Nees, and G. Mourou
CUOS, University of Michigan, Ann Arbor, Michigan 48109

(Received 1 March 2004; accepted 17 June 2004; published 20 August 2004)

Interaction of intense Ti:sapphire laser with solid targets has been studied experimentally by measuring hard x-ray and hot electron generation. Hard x-ray (8–100 keV) emission spectrum and Kα x-ray conversion efficiency (η_K) from plasma have been studied as a function of laser intensity (10^{17}–10^{19} W/cm^2), pulse duration (70–400)fs, and laser pulse fluence. For intensity $I>1\times10^{17}$ W/cm^2, the Ag η_K increases to reach a maximum value of 2×10^{-5} at an intensity $I=4\times10^{18}$ W/cm^2. Hot electron temperature (KT_h) and η_K scaling laws have been studied as a function of the laser parameters. A stronger dependence of KT_h and η_K as a function of the laser fluence than on pulse duration or laser intensity has been observed. The contribution of another nonlinear mechanism, besides resonance absorption, to hard x-ray enhancement has been demonstrated via hot electron angular distribution and particle-in-cell simulations. © *2004 American Institute of Physics*. [DOI: 10.1063/1.1781625]

I. INTRODUCTION

Recent developments of the chirped pulse amplification technique have given access to a new regime of laser-matter interactions with very intense laser fields.[1] The focusing of an ultraintense laser beam on a solid target produces a plasma on its surface. Hot electrons are generated via collective absorption mechanisms, such as resonant absorption[2] (RA) or vacuum heating.[3] They penetrate into the solid target because of the charge separation potential and produce x-ray radiations via K-shell ionizations and bremsstrahlung.[4] This new kind of intense and ultrafast hard x-ray source can be applied to probe matter dynamics on the femtosecond scale.[5] Moreover, because of its small x-ray emission size, it has a number of interesting applications for medical imaging techniques.[6] Further developments of these new x-ray sources are still needed before they can be used in practical applications.

The control and optimization of the x-ray emission of plasmas produced by high intensity laser-solid interaction is a subject of current interest. This requires an understanding of several mechanisms: the laser energy absorption, the hot electron generation, and the x-ray conversion. Several groups have already reported x-ray emission experiments relying on subpicosecond laser systems.[7–13] Earlier works used longer than several hundreds of femtosecond laser pulses produced by CO_2 or Nd laser systems. The ponderomotive force leads to a plasma gradient steeping or to a plasma confinement, satisfying the optimal conditions for resonance absorption. For example, Yu *et al.* systematically studied the hard x-ray emission produced by 500 fs laser pulses[7] and obtained the intensity scaling laws. Soom *et al.* reported high Si and Al Kα conversion yield with 1.3 ps laser.[8] In this experiment, the strong dependence of the Kα emission as a function of the incidence angle and the laser polarization is consistent with the generation of hot electrons by the resonance absorption mechanism. Teubner *et al.*[10] found that additional absorption processes, apart from collisional absorption, are angle and polarization dependent. However, their experiment did not distinguish resonant absorption from vacuum heating. Recently, it was shown that the use of shorter laser pulse durations involve new x-ray emission processes. Eder *et al.* reported the observation of a maximum in Kα x-ray emission when the target is placed away from best focus.[11] They qualitatively explained this result by the reabsorption of the photons produced inside the target. Reich *et al.* theoretically presented a scaling law for optimal laser intensity and predicted a decrease of the hard x-ray yield if the laser intensity is too high.[12] Zhidkov *et al.* studied prepulse effect with a 42 fs laser[13] at moderate intensities and low contrast. This work demonstrated a decrease of the laser energy absorption for this kind of ultrashort pulse durations and also reported the critical influence of the plasma gradient for hot electron generation and hard x-ray emission. Schnürer *et al.* also obtained an x-ray emission decrease[9] by reducing the pulse duration to a value smaller than 120 fs at constant laser energy and target position. No explanations were given and it was suggested that it would need more experimental results. Therefore, in the regime of several tens of femtoseconds, further studies are still necessary to characterize the hard x-ray emission, especially the nature of the energy absorption mechanism.

In this paper, we present and discuss experimental results related to the hard x-ray emission produced by the in-

teraction of ultrashort laser pulse with solid targets. As laser intensity is increasing, the Kα photon conversion efficiency (η_K) keeps on rising and reaches a value as high as 2×10^{-5} for an Ag target at maximum intensity of 4×10^{18} W/cm^2. We observe that this parameter exhibits a stronger dependence as a function of the laser pulse energy than as a function of the laser pulse duration or intensity. Our hot electron measurement proved that other electron heating mechanism, besides resonance absorption, is stimulated and contributes to the x-ray emission enhancement.

II. EXPERIMENTAL SETUP

The experiments are realized with the high intensity INRS Ti:sapphire laser system. The laser delivers maximum output energy of 600 mJ after compression at a repetition rate of 10 Hz and for a 70 fs laser pulse duration. The laser pulse energy can be changed by turning off some of the four laser pumps. The pulse contrast has been measured with a third-order autocorrelator (Sequoia) and is, respectively, 1×10^5 for nanosecond prepulses ($\sim$8 and 16 ns, respectively) and 1×10^4 for picosecond pedestal. The pulse duration is increased by detuning the compressor grating, but then the uncompensated linear phase, or B integral, reduces the pulse contrast down to 1×10^3 for picosecond pedestal with 400 fs pulse duration. The P-polarized laser is focused on the target material at 56° by an $f/3$ parabola mirror with a focal length of 179 mm into a focal spot diameter of 10 μm [full width at half maximum (FWHM)]. A maximum laser intensity of 4×10^{18} W/cm^2 is thus achieved. The target is mounted on a rotary engine to ensure that the laser pulse is incident for each shot on a fresh target. Ag and Cu targets were used in the experiments.

The measurement of the x-ray spectrum and the determination of η_K are made with NaI (Ti) scintillators coupled to a photomultiplier (Philips) used with several pairs of Ross filters.[7] An oscilloscope records the output signal. The whole hard x-ray spectrometer was calibrated using well known γ-ray radiation source ^{241}Am(13.95, 59.54 keV) and ^{133}Ba(30.97, 81.00, 356.00 keV). Some lead shielding is used to minimize the background radiation and a pine hole is put in front of the detector to collimate the x-ray flux, reduce scattering and avoid secondary x-ray radiations. A strong magnetic field, produced with magnets put in front of the detectors, was used to expel electrons from the solid angle of the x-ray detection. A detailed description of this setup can be found in Ref. 7. Moreover, high-resolution line spectra are measured with a cadmium zinc telluride hard x-ray spectrometer.[14]

The x-ray emission size is measured with the knife-edge imaging technique.[7,15] The image magnification factor is equal to 50. The edge-spread function obtained with this technique is fitted with a Fermi function. The differentiation of the Fermi function gives the line-spread function, which can well be fitted by a Gaussian distribution function. The FWHM of this function is defined as the x-ray emisison size.

Recent development of ultrasensitive LiF thermoluminescent dosimeter (TLD) provided thin TLD for hot electron detection.[16] A detector array of this kind (model GR-200F) was used to measure the hot electron angular distribution. TLDs were behind a 1 mm thick Al plate facing the laser target. This diagnostic was placed at different angles from the target normal in the laser incident plane. The electron energy reaching the TLDs was controlled by the thickness of the Al foil before the TLDs and was above 700 keV in our experimental conditions. The background of these TLDs (heat treated at 240 °C) was less than 0.5 nC.

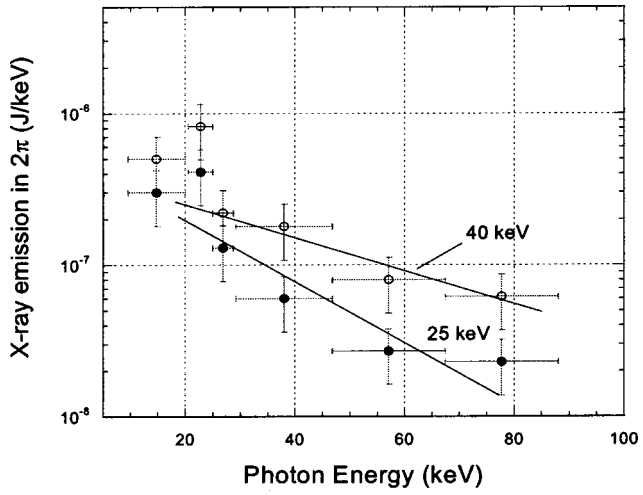

FIG. 1. Hard x-ray spectra produced by a 70 fs laser pulse incident on an Ag target. The laser pulse energy is equal to 460 mJ (open circle) and 260 mJ (solid circle), i.e., respectively, an intensity of 4×10^{18} W/cm^2 and 2.4×10^{18} W/cm^2.

III. HARD X-RAY EMISSION SPECTRA

Figure 1 shows the hard x-ray spectra, measured with NaI scintillators, produced by a laser pulse incident on an Ag bulk target. Spectra have been obtained with 70 fs pulse with 460 and 260 mJ corresponding, respectively, to an intensity $I=4\times10^{18}$ and 2.4×10^{18} W/cm^2. Each spectrum consists of the bremsstrahlung continuous emission and the characteristic Kα line emission. The two spectra exhibit a hot electron temperature (KT_h), respectively, equal to 40 and 25 keV. These values are obtained by fitting the experimental results with a Maxwellian distribution: $f(E)\sim e^{(-E/KT_h)}$.

KT_h scaling law's dependence as a function of the laser intensity were obtained either by changing the laser energy or the pulse duration. At constant laser pulse duration (70 fs), KT_h follows an intensity scaling law that corresponds to $KT_h\sim(I)^{1.0}$, which is very different from typical resonance absorption scaling laws $KT_h\sim(I)^{1/3-1/2}$.[2] At constant laser energy (420 mJ) and for different laser pulse duration, the scaling law exhibits weaker intensity dependence: $KT_h\sim(I)^{0.3}$. This shows that the intensity scaling law dependence of KT_h is more important when we vary the laser fluence at constant pulse duration than when we vary the pulse duration at constant laser energy. This difference in the scaling laws indicates a faster change of the plasma density gradient scale length (and consequently of the energy absorption and plasma thermal temperature) when the fluence is varied at constant pulse duration.

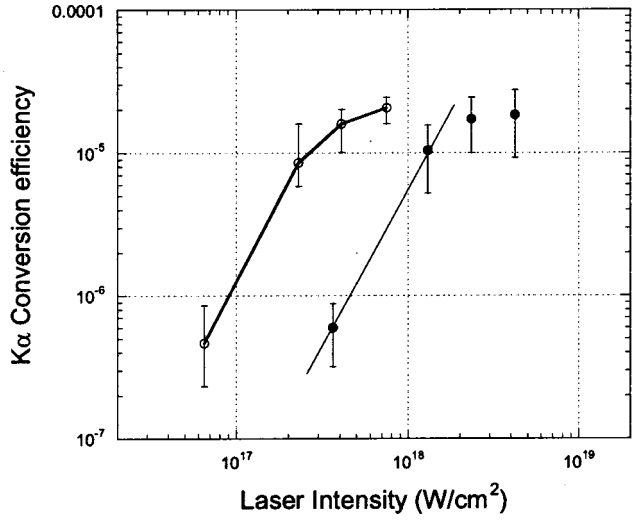

FIG. 2. Ag Kα x-ray conversion efficiency as a function of the laser intensity for a 800 nm laser pulse. 70 fs (solid circle) and 400 fs (open circle) data are presented.

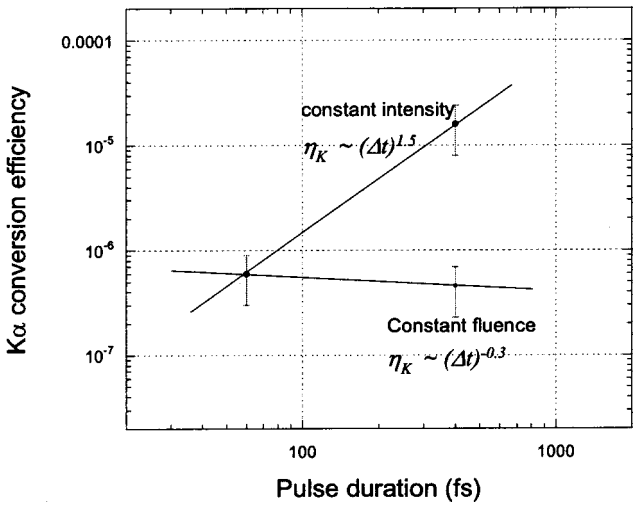

FIG. 3. Kα conversion efficiency dependence as a function of the pulse duration at (a) constant laser intensity ($\sim 7\times10^{17}$ W/cm^2) and (b) constant laser energy (40 mJ).

IV. Kα X-RAY CONVERSION EFFICIENCY

Figure 2 represents the Kα conversion efficiency (η_K) that corresponds to the characteristic hard x-ray emitted in 2π sr by an Ag target, as a function of the laser intensity when we change the laser energy at constant pulse duration of 70 fs (solid circle) or 400 fs (open circle) and constant focal spot size. We observe an increase of η_K with laser energy followed by saturation around $\eta_K = 2\times10^{-5}$ for laser pulse intensities above 1×10^{18} W/cm^2. A similar behavior is observed for both pulse durations. At the intensity corresponding to the maximum of η_K. we also measured the total x-ray conversion efficiency integrated over photon energies above 10 keV and found 4×10^{-4}. We obtain the following scaling law for the Kα photon emission as a function of the laser intensity: $\eta_K \sim (I)^{2.2}$, for an intensity $I \leqslant 10^{18}$ W/cm^2. We should notice that η_K keeps on increasing even at relativistic regime where the x-ray emission is much more intense than the theoretical predications,[12] i.e., η_K starts to drop when $I > 10^{16}$ W/cm^2 for Ag target. The observed saturation of η_K as a function of the laser pulse intensity is directly related to the increase of the hot electron temperature. At higher laser intensity, the hot electrons penetrate more deeply into the solid target and produce the Kα emission far from the target surface. Thus, Kα x-ray photons are reabsorbed between the production point and the target surface, which leads to a saturation of the emission yield.[11,17]

Figure 3 represents η_K as a function of the laser pulse duration at constant spot size: we make a comparison between 400 fs (open circles in Fig. 2) and 70 fs laser pulse durations. At constant laser intensity $I = 7\times10^{17}$ W/cm^2, our experimental results show that a longer pulse duration, corresponding to a longer interaction time, leads to a non-linear increase of the conversion efficiency. The η_K difference between the two laser pulse duration considered is around a factor of 20, which is more important than the linear increment due to the pulse duration increase by a factor of 6. The scaling law dependence of η_K as a function of the pulse duration in that case is $\eta_{ka} = \tau_L^{1.5}$ at a constant laser intensity. It indicates that using longer laser pulse durations increase the plasma scale length and temperature; then it dramatically improves the hard x-ray emission. This scaling law is somewhat similar to what has been obtained in Ref. 18 for soft x-ray emission.

We also studied η_K as a function of the laser pulse duration at constant laser fluence (40 mJ) instead of constant laser intensity. Contrary to what could be expected, we did not observe any important reduction of η_K for a 400 fs compared to a 70 fs laser pulse; even though the laser pulse intensity is higher by a factor of 6 with the shortest laser pulse duration. η_k is roughly constant as a function of the laser pulse duration at constant laser fluence for high laser intensities. The dependence of η_k as a function of the laser pulse duration at constant laser fluence is weaker than at constant laser intensity. It shows that the tendency of the x-ray emission to decrease for the lower laser intensity is greatly compensated for by the use of hundred femtoseconds laser pulse durations. Therefore, in experiments using low contrast 800 nm laser pulses, increasing the laser pulse duration may be an effective way to delay the saturation of the x-ray emission.

Variations of η_K have also been studied as a function of laser intensity, at constant energy and pulse duration, but for different focal spot size[19,20] by varying the relative position of laser focus and target surface. This is another way to study the intensity dependence of the x-ray emission. Focal spot sizes have been measured for each position of the target by an imaging system that includes a microscope objective and a visible charge-coupled derive. Figure 4 shows the dependence of η_K as a function of the laser intensity for 70 fs pulse duration and 420 mJ laser energy (solid line). The dotted line represents the curve obtained for different laser pulse energies at minimum focal spot. We find two interesting phenomena. First, η_K does not show any drop when laser intensity becomes higher than $I_L > 10^{18}$ W/cm^2, which is different from results presented in Refs. 11 and 12. It implies that, in

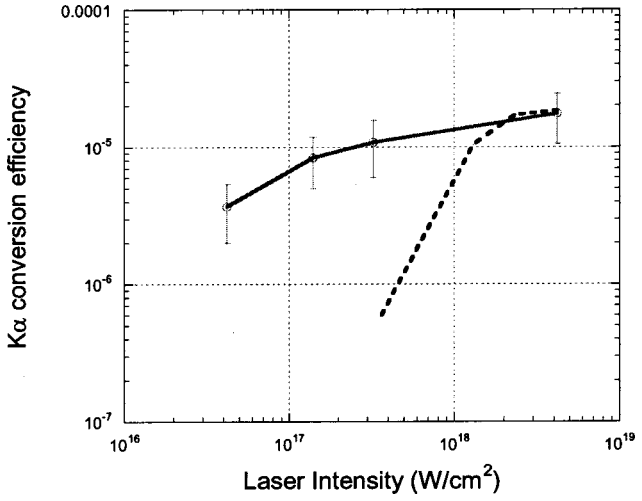

FIG. 4. Kα conversion efficiency as a function of the laser intensity as constant laser pulse duration and energy. The intensity is modified by changing the target position along the focal axis (solid line). The dashed line allows us to do a comparison of η_K evolution in the case where we modify the laser fluence.

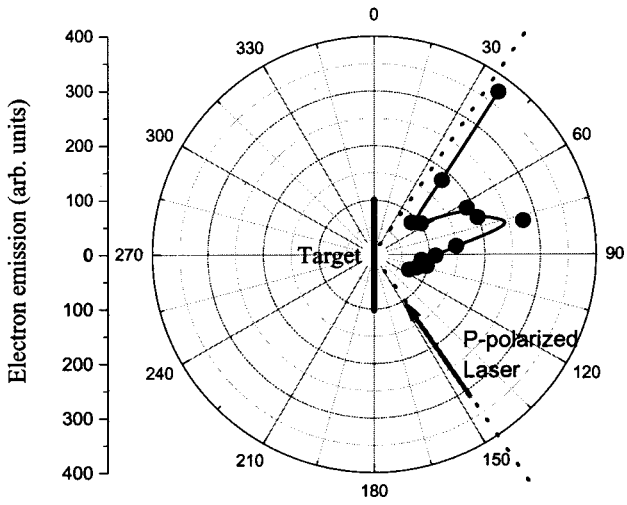

FIG. 5. Angular distribution of the hot electrons (with energy higher than 700 keV) generated by a 4×10^{18} W/cm^2 laser pulse intensity. The data points (solid circle) show the doses measured by the TLDs detector.

our experiment, plasma conditions are very different compared with those already published. Second, the x-ray yield decrease is less important when the intensity is modified by changing the laser focus compared to the case where the laser fluence is varied. At constant laser intensity of $I=4\times10^{17}$ W/cm^2, the difference between the two conversion efficiency is almost one order of magnitude. This observation can be ascribed with the larger emission size. A larger focal spot size and thus a larger emission volume can somewhat compensate the reduction of η_K caused by a lower laser intensity. It shows that the η_K dependence is more important on a change of the laser pulse fluence than on its intensity.

V. HOT ELECTRON ANGULAR DISTRIBUTION

The measure of the angular distribution of outgoing hot electrons generated by laser plasma interaction is very important to determine hot electron heating mechanisms.[21,22] At a laser intensity of $I=4\times10^{18}$ W/cm^2 the angular distribution of the hot electron emission out of the target, with an energy $E>700$ keV, is measured and shown in Fig. 5. We find the presence of two electron peaks of emission going out of the target in the incident plane. One peak is close to the target normal with a difference angle of about 20°.

The other is almost at the laser specular reflection direction. We believe that the first peak is due to the electron heating by resonance absorption, i.e., at the laser reflection point a resonantly enhanced plasma wave accelerates the electrons, through Landon damping or wave breaking, in the direction of the target normal.[2] The emission direction for electrons at constant energy obey the canonical momentum conservation laws[21] described as $\sin\theta'=[(\gamma-1)/\gamma]\sin\theta$, where θ' is the electron emission angle with respect to the target normal, θ is the laser incident angle, and γ is the relativistic factor for hot electrons. The angle we find in our experimental results for 700 keV hot electrons exactly fit this formula. It shows that the resonant absorption mechanism is stimulated in our experimental conditions and that hot electron acceleration is implicated. Similar hot electron emission distribution was also reported by Schwoerer *et al.*[23] They detected an x-ray temperature peak whose direction obeys this law of momentum and energy conservation—free electrons ejected by a ponderomotive force in an underdense plasma. Another mechanism such as vacuum heating[24,25] could also accelerate electron in the same direction, but we do not need to consider it because the plasma scale length L, will be discussed in the following, is much larger than the electron quiver amplitude in the laser field.

The second peak in the specular direction is more attractive because this is the first time it is detected in femtosecond laser plasma interactions. This peak corresponds to a possible stimulation of another mechanism that contributes to the hard x-ray enhancement we observed. The dose value for this peak is even higher than the resonant one. The reflected laser beam contains at least 50% of the incident laser energy,[9] and it can be used to explain the generation of this electron peak. This laser pulse is strong enough to stimulate hot electron relativistic ponderomotive acceleration ($J\times B$), whose energy scales as the ponderomotive potential: $W_{\mathrm{osc}}=(\gamma-1)mc^2$. The value we obtain is almost the same as the electron energy we measured. Other mechanisms such as stimulated Raman scattering (SRS) instability[2,26] might be stimulated also because the laser intensity satisfies the critical intensity for SRS: $I>I_{\mathrm{th}}\sim(4\times10^{17})/L(\mu\mathrm{m})\lambda(\mu\mathrm{m})$ W/cm^2. Especially, relativistic stimulated Raman scattering (RSRS) instability exhibits a high growth rate even at 0.5 n_{cr} and heats electrons in the longitudinal direction.[26] However, in this paper, we do not study these different mechanisms separately. These accelerated hot electrons are then collimated by the quasistatic magnetic channel that occurs simultaneously along the reflected direction in the low-density coronal plasma[21] and formed electron jet emission.

Hot electrons injected into the target, which contribute to the hard x-ray emission, are accelerated by the incident laser

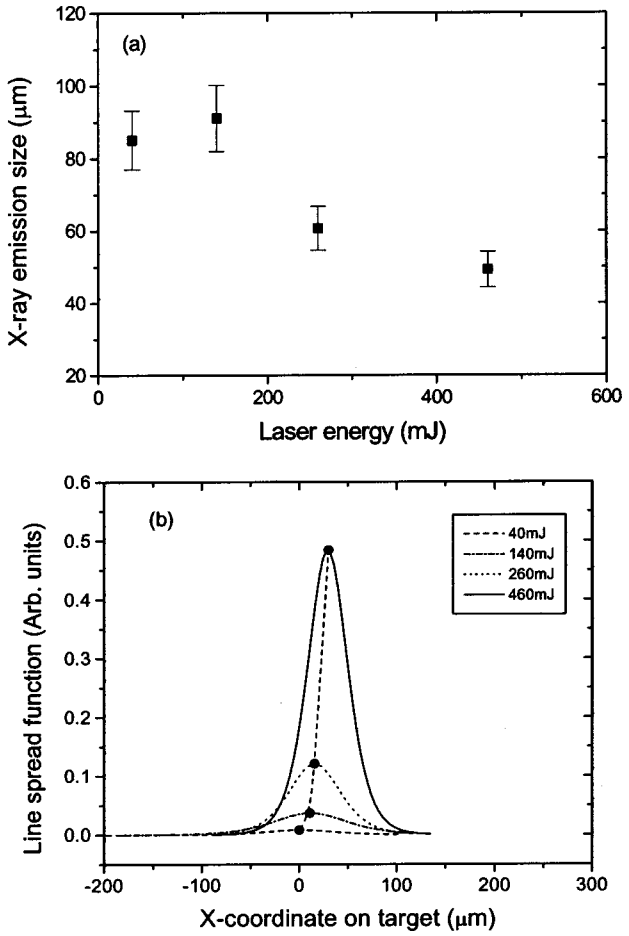

FIG. 6. Hard x-ray emission size as a function of laser energy at 70 fs pulse duration (a) and source position coordinate on target (b).

pulse or the coupling of incident and reflected laser part. The energy of these hot electrons should be higher than the energy of the out-emission electrons because the incident laser energy is more important than the reflected energy. Moreover, the overcritical plasma density stops the plasma wave and allows a more efficient electron $J\times B$ ejection. In the meantime, the surface of the plasma becomes corrugated and the plasma interface is accelerated, which increases the laser energy absorption.[27] Other studies by Sheng *et al.* also define the heating mechanism with low-density plasma coronal as possible stochastic heating because the Raman backscattering wave of a driving pulse can serve as the second counterpropagating pulse to trigger the electron stochastic motion.[28]

VI. HARD X-RAY EMISSION SOURCE SIZE

We measured the hard x-ray emission size as a function of the laser energy with a knife-edge technique [Fig. 6(a)]. The x-ray emission size decreases as the laser intensity becomes higher. It clearly shows the presence of electron pinching at high laser intensities, which contributes to the reduction of the x-ray emission size. A self-generated megagauss magnetic field[29] driven by the Weibel instability may pinch the energetic electron beam. Teng *et al.*[30] observed forward electron jet emission confined by self-generated magnetic field in the target with laser intensity as low as $I\sim 1\times 10^{17}$ W/cm^2. According to Refs. 29–32, the maximum self-generated magnetic field:

$$B_{\max}\approx 230\left(\frac{\eta}{2\times 10^{-6}\ \Omega\ \mathrm{m}}\right)\left(\frac{2\tau}{1\ \mathrm{ps}}\right)\left(\frac{10\ \mu\mathrm{m}}{R}\right)\left(\frac{f_{\mathrm{abs}}}{0.3}\right)\times\left(\frac{I}{10^{17}\ \mathrm{Wcm}^{-2}}\right)^{2/3}\left(\frac{1\ \mu\mathrm{m}}{\lambda}\right)^{2/3}\ \mathrm{T}$$

in which plasma resistivity $\eta=[5\times 10^6(KT)^{-1}+170(KT)^{3/2}+3\times 10^5]^{-1}\Omega$ m and other parameters are defined in Ref. 31. In our experiment, it is about 40 MG with the highest laser intensity if we choose an energy absorption of about 30%. Therefore, for the electron emission out of target, this multimegagauss quasistatic magnetic field excited in front of the target pinch the outgoing electron stream. Simulation results[21] with laser intensity $I\sim 2x10^{18}$ W/cm^2 show that a low-density plasma coronal plays an important role in forming the electron jet, without which no out-emission jet is observed. In our experiment, as laser energy increases, two prepulses with intensity $I>10^{13}$ W/cm^2 at 8 and 16 ns before the main pulse, respectively, start to produce a long plasma coronal before main pulse arrives as stated by Ref. 32. Therefore, hard x-ray emission source size reduction demonstrates the stimulation of the self-generated magnetic field and *the existence of this long length plasma coronal*. If the laser intensity drops, the magnetic field quickly decreases, which enlarges the emission size, as our experiment shows.

It is interesting to notice the movement of x-ray emision center as a function of laser pulse energy. As shown in Fig. 6(b), x-ray emission center displacement on target was 30 μm if we compare 460 mJ laser incident energy with 40 mJ case. It shows the critical surface extension is larger than 15 μm. According to scale length definition, the plasma scale length is larger than 3 if the solid density is 100 n_{cr}.

VII. PIC SIMULATIONS

Simulations using a 1D fully electromagnetic LPIC++ code[33] have been performed, where an electromagnetic wave is launched obliquely at 56° onto an over dense plasma. In the simulations we use the following parameters: $n_e/n_c=20, T_e=100$ eV, $T_e/T_i=3-5$, and the mass ratio $m_i/Zm_e=1836$. The initial scale length (L/λ) is varied from 0 to 10. The incident laser pulse is a square-sine profile that lasts 30 laser cycles. The dimensionless field amplitude $a=eE_0/m_e\omega c=0.9$ is used. Typically 50 electrons and ions per cells and 1700 cells are used. We consider the initial situation in which the ions are mobile and electrons are pulled out into vacuum by the component of electrical field normal to the target. Figure 7 shows the integrated electron energy obtained as a function of the plasma density gradient L/λ from 0 to 10 ($\Delta t=30$ laser cycles, $a=0.9$). In this range, there are four absorption peaks, respectively, at scale length $L/\lambda=0.1, 0.25, 0.6$, and $3-6$. The first one corresponds to the contribution of vacuum heating.[24] According to our optimal scale length estimation, the second peak corresponds to resonant absorption. The fourth peak, which corresponds to our

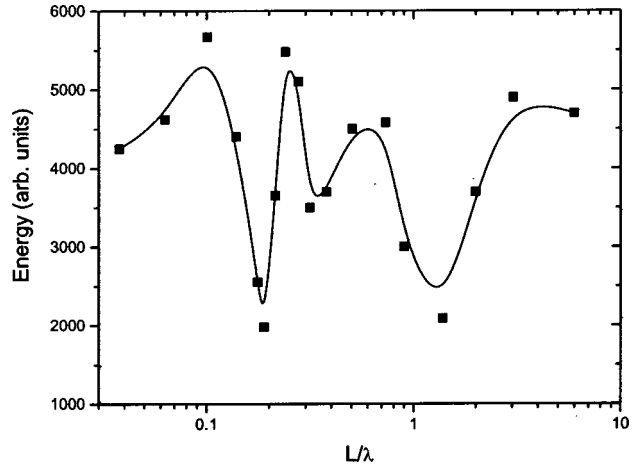

FIG. 7. Integrated electron energy absorbed as a function of the density gradient (L/λ). The laser pulse is P polarized and is incident on the target at 56°, it contains 30 optical cycles and the dimensionless amplitude is $a=0.9$.

experimental conditions, exhibits laser energy absorption as strong as the resonant one. Figure 8 shows the electron velocity distribution at $t=10$ laser cycles for a plasma scale length, respectively, of $L/\lambda=0.25$ [Fig. 8(a)] and 3 [Fig. 8(b)], the other laser parameters are kept constant. Although the energy laser absorption and the electron spectra for both scale length are almost the same at $t=30$, the spectrum obtained at $t=10$ for $L/\lambda=3$ exhibits a much higher electron heating than in the case of $L/\lambda=0.25$ which is optimal for RA. It proves that the stimulation of a resonant plasma wave takes many laser cycles,[34] then this large amplitude electric field localized at the critical surface breaks to accelerate electrons. By the way, if we compare v_y, the electronic speed along the plasma surface, in Figs. 8(a) and 8(b), this variable is greatly enhanced in the case of long scale length, which shows that electron acceleration does not concentrate only in the target normal direction (v_x). This phenomenon confirms what we found about hot electron jet emission in our experiment.

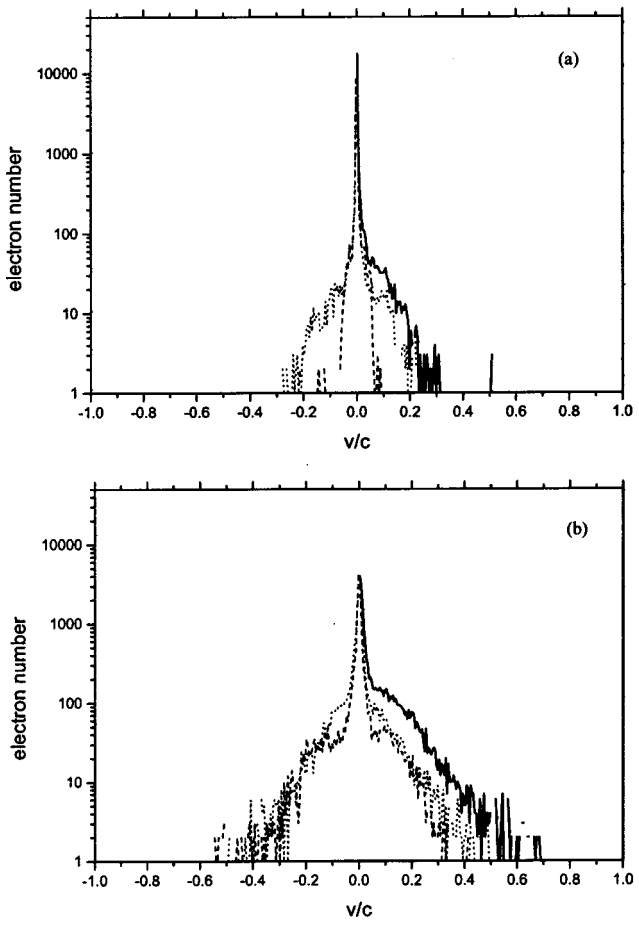

FIG. 8. Electrons velocity distribution at $t=10$ laser cycles in the laboratory frame for $L/\lambda=0.25$ (a) and 3 (b). The numbers of electrons as a function of v_x (dotted line), v_y (dashed line), and $v=\sqrt{v_x^2+v_j^2+v_x^2}$ (solid line) are presented.

VIII. DISCUSSION

We have noticed that η_K keeps increasing when the laser intensity becomes higher. This observation does not fit with the theoretical prediction of Ref. 12 for the same target and pulse duration where the intensity at which η_K saturates is about 10^{16} W/cm^2 for Ag target. Our experimental data exhibit much higher saturation laser intensity above 10^{18} W/cm^2. We can explain this discrepancy by using the plasma scale length L because the hot electron generation will be greatly affected by this parameter when different laser pulse contrasts and energies are considered.[2,3] The optimal L for resonance absorption is given by $(2\pi L/\lambda)^{2/3}\sin^2\theta\approx 0.6$, where θ is the incident angle to the target normal. Parameters of simulation in Ref. 12 satisfy this formula because a high contrast 60 fs pulse was considered, and the plasma scale length was fixed to 0.3λ. The predictions of this publication were totally based on this assumption. On the contrary in our experiment, L at the critical density is intensity dependent and is superior to 3λ according to Refs. 13 and 32 and to our measurements. This value is far away from the optimal scale length for RA. However, according to our simulation and Refs. 13 and 24, this increment of RA will be greatly reduced by the use of an ultrashort pulse duration (70 fs) because the production of a resonant plasma wave at the critical surface is a slow many-cycle buildup which put off the plasma wave to eventually breaks.[24,25] On the other hand, the hot electrons produced by short duration laser pulse exhibits a high temperature that is not suitable for Kα production[9,11] if we compare it to 400 fs laser pulse at constant laser energy. All of these reasons imply Kα emission is not greatly enhanced with relativistic 70 fs laser pulse irradiation. This conclusion is yet contrary to our experimental results that demonstrate an enhancement of the x-ray emission at high intensities. Therefore, some other mechanisms, such as relativistic ponderomotive force followed by $J\times B$ electron forward acceleration or RSRS, are stimulated and increase the hot electron generation in the high intensity regime. This conclusion is consistent with the measurement of hot electron angular distribution.

From the above analysis, it is easy to understand the second unique phenomenon observed in our experiments: KT_h and η_K both depend more importantly on laser fluence

than on pulse duration and intensity. Because $J \times B$ is sensitive to laser intensity (I) and plasma scale length (L), increasing the laser fluence with the same pulse shape, corresponds to increase in both of these two parameters. So, η_K will nonlinearly increase in this case. However, if the laser fluence is kept constant and the pulse duration is shortened to 70 fs, the laser intensity I is increased as usual. But in the meantime, the laser contrast rises from 10^3 to 10^4 for picosecond pedestal. It means the pedestal of the laser pulse becomes much narrow because we lose the nonlinear pulse chirp. In this way, the increment of the plasma scale length L due to the higher laser intensity of the pedestal is greatly compensated by the higher pulse contrast. Therefore, the x-ray emission enhancement is very limited compared with the case where we increase the laser fluence.

IX. CONCLUSIONS

Hard x-ray ($8-100$ keV) emission spectrum and Kα x-ray conversion efficiency (η_K) from plasma produced by irradiation of a femtosecond Ti: sapphire laser on a solid target have been studied as a function of laser intensity (10^{17}–10^{19} W/cm^2), pulse duration ($70-400$ fs), and laser pulse fluence. For intensity $I > 1 \times 10^{17}$ W/cm^2, the Ag η_K increases to reach a maximum value of 2×10^{-5} at an intensity $I = 4 \times 10^{18}$ W/cm^2. We found that η_K is more importantly dependent on laser fluence than on pulse duration or laser intensity. Large plasma scale length is the key factor that contributes to these phenomena. Pinching of the x-ray source size demonstrated the existence of a long low-density plasma coronal. Hot electron angular distribution proved that another nonlinear mechanism is stimulated besides resonance absorption which is not effective anymore in femtosecond regime. We suggest the use of high contrast double frequency laser pulse in future experiments to precisely control the plasma expansion and the x-ray generation.

ACKNOWLEDGMENTS

The authors would like to acknowledge the help in experiment provided by R. Toth and the technical support of F. Poitras and C. Sirois.

This work was supported by the Natural Science and Engineering Research Council of Canada and the Michigan Economic Development Corporation's MLSC (Grant No. 0085P1001461).

[1] M. D. Perry and G. Mourou, Science **264**, 917 (1994); D. Strickland and G. Mourou, Opt. Commun. **56**, 219 (1985).
[2] W. L. Kruer, *The Physics of Laser Plasma Interactions* (Addison-Wesley, New York, 1988); N. H. Burnett and G. D. Enright, Can. J. Chem. **64**, 920 (1986).
[3] F. Brunel, Phys. Rev. Lett. **59**, 52 (1987); L. M. Chen, J. Zhang, Q. L. Dong, H. Teng, T. J. Liang, L. Z. Zhao, and Z. Y. Wei, Phys. Plasmas **8**, 2925 (2001).
[4] H. Chen, B. Soom, B. Yaakobi, S. Uchida, and D. D. Meyerhofer, Phys. Rev. Lett. **70**, 3431 (1993); T. Feurer, W. Theobald, R. Sauerbrey *et al.*, Phys. Rev. E **56**, 4608 (1997).
[5] J. C. Kieffer, M. Chaker, J. P. Matte *et al.*, Phys. Fluids B **5**, 2676 (1993).
[6] J. C. Kieffer, A. Krol, Z. Jiang, C. Chamberlain, E. Scalzetti, and Z. Ichalalene, Appl. Phys. B: Lasers Opt. **74**, 75 (2002).
[7] J. Yu, Z. Jiang, J. C. Kieffer, and A. Krol, Phys. Plasmas **6**, 1318 (1999).
[8] B. Soom, H. Chen, Y. Fisher, and D. D. Meyerhofer, J. Appl. Phys. **74**, 5372 (1993).
[9] M. Schnürer, R. Nolte, A. Rousse, G. Grillon, G. Cheriaux, M. P. Kalachnikov, P. V. Nickles, and W. Sandner, Phys. Rev. E **61**, 4394 (2000).
[10] U. Teubner, J. Bergmann, B. van Wonterghem, F. P. Schäfer, and R. Sauerbrey, Phys. Rev. Lett. **70**, 794 (1993); U. Teubner, I. Uschmann, P. Gibbon *et al.*, Phys. Rev. E **54**, 4167 (1996).
[11] D. C. Eder, G. Pretzler, E. Fill, K. Eidmann, and A. Saemann, Appl. Phys. B: Lasers Opt. **70**, 211 (2000).
[12] C. Reich, P. Gibbon, I. Uschmann, and E. Forster, Phys. Rev. Lett. **84**, 4846 (2000).
[13] A. Zhidkov, A. Sasaki, T. Utsumi *et al.*, Phys. Rev. E **62**, 7232 (2000).
[14] L. M. Chen, P. Forget, R. Toth *et al.*, Rev. Sci. Instrum. **74**, 5035 (2003).
[15] K. Chu and A. Fenster, Med. Phys. **10**, 772 (1983).
[16] L. M. Chen, J. J. Park, K.-H. Hong, J. L. Kim, J. Zhang, and C. H. Nam, Phys. Rev. E **66**, 025402 (2002); L. M. Chen, J. Zhang, H. Teng, Q. L. Dong, Z. L. Chen, T. J. Liang, L. Z. Zhao, and Z. Y. Wei, *ibid.* **63**, 036403 (2001).
[17] D. Salzmann, C. Reich, I. Uschmann, and E. Forster, Phys. Rev. E **65**, 036402 (2002).
[18] D. Altenbernd *et al.*, J. Phys. B **30**, 3969 (1997).
[19] G. Pretzler, F. Brandl, J. Stein, E. Fill, and J. Kuba, Appl. Phys. Lett. **82**, 3623 (2003).
[20] E. Esarey, P. Sprangle, J. Krall, and A. Ting, IEEE J. Quantum Electron. **33**, 1879 (1997).
[21] Y. Sentoku, H. Ruhl, K. Mima, R. Kodama, K. A. Tanaka, and Y. Kishimoto, Phys. Plasmas **6**, 2855 (1999).
[22] L. M. Chen, J. Zhang, Y. T. Li *et al.*, Phys. Rev. Lett. **87**, 225001 (2001); D. F. Cai, Y. Q. Gu, Z. J. Zheng, T. S. Wen, S. T. Chunyu, Z. B. Wang, and X. D. Yang, Phys. Plasmas **10**, 3265 (2003).
[23] H. Schwoerer, P. Gibbon, S. Dusterer, R. Behrens, C. Ziener, C. Reith, and R. Sauerbrey, Phys. Rev. Lett. **86**, 2317 (2001).
[24] P. Gibbon and A. R. Bell, Phys. Rev. Lett. **68**, 1535 (1992); **73**, 664 (1994).
[25] M. K. Grimes, A. R. Rundquist, Y. S. Lee, and M. C. Downer, Phys. Rev. Lett. **82**, 4010 (1999).
[26] J. C. Adams, A. Heron, S. Guerin, G. Laval, P. Mora, and B. Quesnel, Phys. Rev. Lett. **78**, 4765 (1997).
[27] S. C. Wilks, W. L. Kruer, M. Tabak, and A. B. Langdon, Phys. Rev. Lett. **69**, 1383 (1992).
[28] Z. M. Sheng, Y. Sentoku, K. Mima, J. Zhang, W. Yu, and J. Meyer-ter-Vehn, Phys. Rev. Lett. **85**, 5340 (2000).
[29] V. A. Vshivkov, N. M. Naumova, F. Pegoraro, and S. V. Bulanov, Phys. Plasmas **5**, 2727 (1998).
[30] H. Teng, J. Zhang, Z. L. Chen, Y. T. Li, K. Li, X. Y. Peng, and J. X. Ma, Phys. Rev. E **67**, 026408 (2003).
[31] J. R. Davies, A. R. Bell, and M. Tatarakis, Phys. Rev. E **59**, 6032 (1999).
[32] C. Ziener, I. Uschmann, G. Stobrawa *et al.*, Phys. Rev. E **65**, 066411 (2002).
[33] R. Lichters, J. Meyer-ter-Vehn, and A. Pukhov, Phys. Plasmas **3**, 3425 (1996).
[34] J. P. Freidberg, R. W. Mitchell, R. L. Morse, and L. I. Rudsinski, Phys. Rev. Lett. **28**, 795 (1972).